

# On XCP Stability in a Heterogeneous Network

Yusuke Sakumoto, Hiroyuki Ohsaki, and Makoto Imase  
Graduate School of Information Science and Technology  
Osaka University, Suita, Osaka 565-0871, Japan  
{y-sakumt,oosaki,imase}@ist.osaka-u.ac.jp

## Abstract

*In this paper, we analyze stability of XCP (eXplicit Control Protocol) in a network with heterogeneous XCP flows (i.e., XCP flows with different propagation delays). Specifically, we model a network with heterogeneous XCP flows using fluid-flow approximation. We then derive the conditions that XCP control parameters should satisfy for stable XCP operation. Furthermore, through several numerical examples and simulation results, we quantitatively investigate effect of system parameters and XCP control parameters on stability of the XCP protocol. Our findings include: (1) when XCP flows are heterogeneous, XCP operates more stably than the case when XCP flows are homogeneous, (2) conversely, when variation in propagation delays of XCP flows are very large, operation of XCP becomes less stable, and (3) output link bandwidth of an XCP router is independent of stability of the XCP protocol.*

## 1 Introduction

In recent years, exploitation of the network in larger capacity and wider region has rapidly been in progress. In an experimental testbed network, bandwidth reaches several tens of Gbit/s and the transmission delay between end hosts sometimes reaches a hundred msec [13, 17].

TCP (Transmission Control Protocol) has been widely used in the Internet to carry data traffic [11]. There are various versions of TCP, and the most popular ones are TCP version Reno (TCP Reno) and its variants [10]. Several problems of TCP Reno have been reported such as its inability to support rapidly increasing speeds of recent networks [1, 3, 14].

One of serious problems in TCP Reno is that a large number of packets sent into the network are discarded. This problem is caused by inability of source hosts to detect congestion before some packets are lost, and large delay for source hosts to detect congestion when the round-trip time between end hosts is large. Since the scale and the speed of network is continuously increasing, it is expected that the performance of TCP Reno would be further degraded due to increased number of packet losses before source hosts'

congestion detection.

For solving such problems in a high-speed and wide-area network, many transport-layer communication protocols using explicit feedback from a router to end hosts are proposed [6, 12, 15, 16]. Compared with TCP Reno, these protocols perform efficient congestion control between end hosts with the aid of routers. Among those router-assisted congestion control mechanisms, XCP (eXplicit Control Protocol) has been receiving attention [2, 6]. XCP is a sort of window-based flow control mechanisms. An XCP router periodically calculates the amount of window size increase/decrease for a source host, and notifies source hosts of it as explicit feedback. With such explicit feedback, an XCP source host can quickly and appropriately respond to congestion status of the network.

By simulation experiments, it has been reported that XCP achieves better performance than TCP Reno does [5, 6]. However, characteristics of XCP as a feedback-based control system, such as stability and transient performance, have not been sufficiently clarified. There exist several analytical studies on XCP using fluid-flow approximation [6, 7, 18]. In [6], by assuming an identical propagation delay for all XCP flows, stability of XCP has been analyzed. The authors of [6] have derived a sufficient condition for XCP control parameters to stabilize XCP's operation. Similar to [6], in [18], by assuming an identical propagation delay for all XCP flows, stability of XCP has been analyzed. By extending the analytic model in [6], the authors of [18] have shown that operation of XCP becomes unstable when the available bandwidth of an XCP router's output link is not fixing. However, in real networks, propagation delays of XCP flows must not be the same. In the literature, effect of the difference in propagation delays of XCP flows on stability of XCP protocol has not been clarified. In [7], steady state performance of XCP in a tandem network (i.e., a network with multiple routers) has been analyzed. Specifically, the authors of [7] have derived throughput of XCP flows in steady state, and have shown that fairness among XCP flows is significantly degraded unless control parameters of an XCP router are configured appropriately. Although multiple XCP flows with different propagation delays are modeled in [7], stability of XCP has not been investigated.

In this paper, we analyze stability of XCP in a network with heterogeneous XCP flows (i.e., XCP flows with differ-

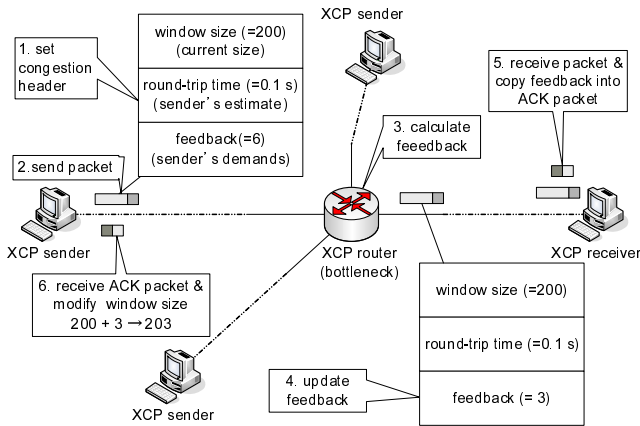


Figure 1: Overview of XCP's congestion control using congestion header of packets

ent propagation delays). Specifically, we model a network with heterogeneous XCP flows using fluid-flow approximation. We then derive the conditions that XCP control parameters should satisfy for stable XCP operation. Through several numerical examples and simulation results, we quantitatively investigate effect of system parameters and XCP control parameters on stability of the XCP protocol. Our findings include: (1) when XCP flows are heterogeneous, XCP operates more stably than the case when XCP flows are homogeneous, (2) conversely, when variation in propagation delays of XCP flows are very large, operation of XCP becomes less stable, and (3) the output link bandwidth of an XCP router is independent of stability of the XCP protocol.

The organization of this paper is as follows. First, in Section 2, the algorithm of XCP operation is briefly explained. In Section 3, heterogeneous XCP connections and an XCP router are modeled using fluid-flow approximation. Section 4 performs stability analysis of XCP. In Section 5, the effect of system parameters and XCP control parameters on stability of the XCP protocol is quantitatively evaluated by presenting several numerical examples and simulation results. Finally, in Section 6, we conclude this paper and discuss future works.

## 2 XCP (eXplicit Control Protocol)

In this section, the congestion control algorithm of XCP is briefly summarized. Refer to [6] for details of the XCP algorithm.

In XCP, congestion information is exchanged between a source host and a router using *congestion header* in a packet. An overview of the XCP congestion control using the congestion header of a packet is illustrated in Fig. 1.

XCP is a sort of window-based flow control mechanisms. In XCP, a router calculates the amount of window size increase/decrease for a source host, and it then notifies the

source host of the calculated value as explicit feedback. The congestion header of a packet stores information on a source host and a router: e.g., the window size and the estimated round-trip time of the source host, and the amount of window-size increase/decrease (feedback value) calculated by the router.

At the time of packet transmission, a source host stores its estimated round-trip time, its current window size, the initial value of the feedback value (i.e., the amount of window size increase requested by the source host) in the congestion header of the packet. This enables the XCP router to know the status of the source host.

When the packet arrives at an XCP router, the router calculates a feedback value based on the information stored in the congestion header of the packet. The router overwrites the feedback value in the congestion header of the packet with the calculated feedback value, if the feedback value stored in the congestion header is larger than the calculated feedback value. The XCP router then forwards the packet to its downstream router.

Once the packet arrives at a destination host, the destination host returns an ACK (ACKnowledgement) packet to the source host. At this time, the congestion header of the data packet is copied to the congestion header of the ACK packet. This makes it possible for the source host to know the congestion information of XCP routers by way of the destination host.

Finally, when the source host receives the ACK packet, the feedback value stored in the congestion header of the ACK packet is added to the current window size of the source host.

In what follows, we explain how an XCP router calculates a feedback value (i.e., the amount of increase/decrease of the window size of a source host).

The control mechanism of an XCP router is composed of *efficiency controller*, which tries to maximize utilization of the router, and *fairness controller*, which tries to realize fairness among competing XCP flows. The efficiency controller and the fairness controller are invoked every the average round-trip time of all XCP flows. The efficiency controller calculates the total amount of rate increase/decrease for all XCP flows. The fairness controller then calculates the amount of rate increase/decrease for each XCP flow. An XCP router calculates a feedback value based on the amount of rate increase/decrease calculated by the fairness controller and information stored in the congestion header of arriving packets. In what follows, algorithms of the efficiency controller and the fairness controller are briefly explained.

The efficiency controller calculates the aggregate feedback value  $\phi$  (i.e., the total amount of rate increase/decrease for all XCP flows) from the packet arrival rate at the XCP router and the current queue length as

$$\phi = \alpha d S - \beta Q, \quad (1)$$

where  $d$  is the average round-trip time of XCP flows accommodated in the XCP router,  $S$  is the available bandwidth of

the link (i.e., the output link bandwidth excluding the current packet arrival rate),  $Q$  is the minimum queue length observed during the average round-trip propagation time, and  $\alpha$  and  $\beta$  are control parameters of the XCP router.

The fairness controller distributes the aggregate feedback value  $\phi$  to all XCP flows. The fairness controller realizes fairness among XCP flows by performing an AIMD (Additive Increase and Multiplicative Decrease) control. Namely, the fairness controller equally distributes  $\phi$  to all XCP flows when  $\phi \geq 0$ . On the contrary, when  $\phi < 0$ , the fairness controller distributes  $\phi$  to all XCP flows, such that the bandwidth allocation to each XCP flow is proportional to its throughput. Specifically, the fairness controller calculates  $\xi_p$  and  $\xi_n$ , which are used for calculating the feedback value.

$$\xi_p = \frac{h + [\phi]^+}{d \sum_{k=1}^N \frac{rtt_k s_k}{w_k}} \quad (2)$$

$$\xi_n = \frac{h + [-\phi]^+}{dT} \quad (3)$$

In the above equations,  $N$  is the number of packets arrived at the XCP router during the average round-trip time  $d$ , and  $T$  is the total size of the arrived packets. Also,  $w_k$  and  $rtt_k$  are the window size and the estimated round-trip time stored in the congestion header of the  $k$ -th packet, and  $s_k$  is the packet size of the  $k$ -th packet. Note that  $[x]^+ \equiv \max(x, 0)$ .

In Eq. (3),  $h$  is called *shuffle traffic*, and is determined by

$$h = [\gamma T - |\phi|]^+, \quad (4)$$

where  $\gamma$  is a control parameter of an XCP router.

Finally, an XCP router calculates the feedback value  $H_{feedback_k}$  for the  $k$ -th packet as

$$H_{feedback_k} = \xi_p \frac{rtt_k^2 s_k}{w_k} - \xi_n rtt_k s_k. \quad (5)$$

### 3 Modeling with Fluid-Flow Approximation

In this paper, we model a network with heterogeneous XCP flows with different propagation delays (i.e., XCP flows traversing links with different propagation delays) sharing the single bottleneck link as a discrete-time system (Fig. 2). XCP flows are classified into *flow classes*, in which XCP flows have the identical propagation delay. In our analysis, dynamics of transfer rates from XCP flows, and the queue length of an XCP router are modeled as discrete-time models with slot length of  $\Delta$ . The definition of symbols used throughout our analysis is summarized in Tab. 1.

First, we model dynamics of the transfer rate from an XCP flow. In our analysis, we assume: (1) all XCP flows with the same propagation delay synchronize, (2) all XCP source hosts always have data to transfer, (3) sizes of all packets are equal, (4) the window size of a source host is changed only by receiving the feedback value from XCP routers (i.e., effect of timeouts triggered by a large number

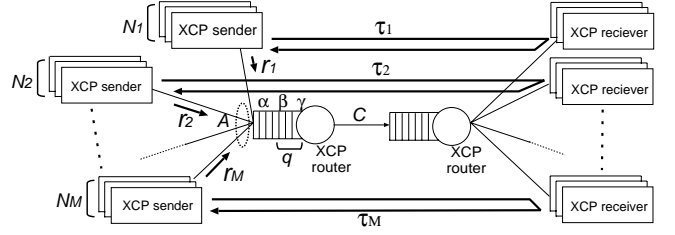


Figure 2: Analytic model

Table 1. The definition of symbols

$M$	the number of flow classes
$N_i$	the number of XCP flows in flow class $i$
$\Delta$	slot length
$r_i$	transfer rate of XCP flows in flow class $i$
$\tau_i$	two-way propagation delay of XCP flows in flow class $i$
$\tau$	average round-trip time $\tau$ of all XCP flows
$s$	packet length
$q$	current queue length of XCP router
$\phi$	aggregate feedback of XCP router
$h$	shuffle traffic of XCP router
$A$	packet arrival rate at XCP router
$C$	output link bandwidth of XCP router
$\alpha$	XCP control parameter
$\beta$	XCP control parameter
$\gamma$	XCP control parameter

of packet losses are negligible), and (5) the round-trip time of an XCP flow is equal to its two-way propagation delay.

Since an XCP router performs the same congestion control for all XCP flows with the same round-trip time (see Eq. (5)), the assumption (1) is reasonable. Moreover, since XCP is mainly used for transferring a large amount of data in a high-speed network, assumptions (2) through (4) should be appropriate. The assumption (5) is reasonable since the control objective of an XCP router is to minimize its queue length, resulting negligible queuing delay at the router buffer. The transfer rate and the two-way propagation delay of XCP flows in flow class  $i$  are denoted by  $r_i$  and  $\tau_i$ , respectively. Moreover, the number of XCP flows in flow class  $i$  is denoted by  $N_i$ . Then, the packet arrival rate  $A$  at an XCP router and the average round-trip time  $\tau$  of all XCP flows are given by

$$A = \sum_{i=1}^M N_i r_i, \quad (6)$$

$$\tau = \frac{\sum_{i=1}^M N_i \tau_i}{\sum_{i=1}^M N_i}. \quad (7)$$

Since  $\sum_{k=1}^N rtt_k s_k / w_k \simeq d \sum_{i=1}^M N_i$  in Eq. (2) [7] and

$T \simeq A\tau$ ,  $\xi_p$  and  $\xi_n$  (Eqs. (2) and (3)) are given by

$$\xi_p = \frac{h + [\phi]^+}{\tau^2 \sum_{i=1}^M N_i}, \quad (8)$$

$$\xi_n = \frac{h + [-\phi]^+}{\tau^2 A}. \quad (9)$$

In the above equations, the aggregate feedback value  $\phi$  and the shuffle traffic  $h$  are given by Eqs. (1) and (4) as

$$h = [\gamma\tau A - |\phi|]^+, \quad (10)$$

$$\phi = \alpha\tau(C - A) - \beta q, \quad (11)$$

where  $q$  is the current queue length of the XCP router, and  $C$  is the output link bandwidth of the XCP router.

From Eqs. (5) through (9), the feedback value  $H_{feedback_i}$  for XCP flows in flow class  $i$  is given by

$$H_{feedback_i} = \frac{h + [\phi]^+}{\tau^2 \sum_{j=1}^M N_j} \frac{\tau_i s}{r_i} - \frac{h + [-\phi]^+}{\tau^2 A} \tau_i s. \quad (12)$$

Hence, at the time of ACK packet reception, the amount of change in the transfer rate of XCP flows in flow class  $i$  is given by

$$\frac{H_{feedback_i}}{\tau_i} = \frac{h + [\phi]^+}{\tau^2 \sum_{j=1}^M N_j} \frac{s}{r_i} - \frac{h + [-\phi]^+}{\tau^2 A} s. \quad (13)$$

The transfer rate of XCP flows in flow class  $i$  and the current queue length of the XCP router at slot  $k$  are denoted by  $r_i(k)$  and  $q(k)$ , respectively. Without loss of generality, we assume that the propagation delay from a source host to the XCP router is zero, and that the propagation delay from the XCP router to source hosts by way of the destination hosts is  $\tau_i$ . The information stored in the congestion header of the ACK packet received by a source host at slot  $k$  is  $k - \tau_i/\Delta$  slots old. Moreover, the number of ACK packets that a source host receives during the slot length  $\Delta$  can be approximated by  $r_i(k - \tau_i/\Delta) \Delta/s$ . Thus, from Eq. (13), the transfer rate of XCP flows in flow class  $i$  at  $(k+1)$ -th slot is given by

$$r_i(k+1) \simeq r_i(k) + \Delta \frac{h(k - \frac{\tau_i}{\Delta}) + [\phi(k - \frac{\tau_i}{\Delta})]^+}{\tau^2 \sum_{j=1}^M N_j} - \Delta \frac{r_i(k - \frac{\tau_i}{\Delta}) (h(k - \frac{\tau_i}{\Delta}) + [-\phi(k - \frac{\tau_i}{\Delta})]^+)}{\tau^2 A(k - \frac{\tau_i}{\Delta})}. \quad (14)$$

Next, we model the dynamics of the queue length of an XCP router. Letting  $q(k)$  be the current queue length of the XCP router at slot  $k$ , the current queue length  $q(k+1)$  at slot  $k+1$  is approximately given by

$$q(k+1) \simeq \begin{cases} q(k) + \Delta (A(k) - C) & \text{if } q(k) > 0 \\ q(k) + \Delta [A(k) - C]^+ & \text{if } q(k) = 0 \end{cases}. \quad (15)$$

## 4 Stability Analysis

In what follows, using the fluid-flow approximation model of XCP derived in Section 3, we analyze the stability (local asymptotic stability) of XCP around its equilibrium point using the same analytic approach with [4]. In what follows, equilibrium values of the transfer rate  $r_i(k)$  and the current queue length  $q(k)$  are denoted by  $r_i^*$  and  $q^*$ , respectively. First, we linearize the fluid-flow approximation model defined by Eqs. (14) and (15) at its equilibrium point. Since the aggregate feedback value  $\phi(k)$  and the current queue length  $q(k)$  are discontinuous at the equilibrium point (i.e.,  $\phi^* = 0$  and  $q^* = 0$ ), we introduce the following approximation with  $f(x) = 0$  and  $\Delta \ll 1$ .

$$\frac{[f(x + \Delta)]^+ - [f(x)]^+}{\Delta} \simeq \frac{1}{2} \frac{f(x + \Delta) - f(x)}{\Delta} \quad (16)$$

Thereby, Eqs. (14) and (15) can be approximated as

$$r_i(k+1) \simeq r_i(k) + \Delta \frac{h(k - \frac{\tau_i}{\Delta}) + \phi(k - \frac{\tau_i}{\Delta})/2}{\tau^2 \sum_{j=1}^M N_j} - \Delta \frac{r_i(k - \frac{\tau_i}{\Delta}) (h(k - \frac{\tau_i}{\Delta}) - \phi(k - \frac{\tau_i}{\Delta})/2)}{\tau^2 A(k - \frac{\tau_i}{\Delta})}, \quad (17)$$

$$q(k+1) \simeq q(k) + \frac{\Delta (A(k) - C)}{2}. \quad (18)$$

These equations suggest that state variables at slot  $k+1$  are determined by state variables from  $k - \nu$  ( $\nu \equiv \max_{1 \leq i \leq M} \tau_i/\Delta$ ) to slot  $k$ . Furthermore, we linearize Eq. (17) around its equilibrium point as

$$r_i(k+1) \simeq \sum_{m=1}^M \sum_{n=0}^{\nu} \frac{\partial r_i(k+1)}{\partial r_m(k-n)} \{r_m(k-n) - r_m^*\} + \sum_{n=0}^{\nu} \frac{\partial r_i(k+1)}{\partial q(k-n)} \{q(k-n) - q^*\}. \quad (19)$$

We introduce a state vector  $\mathbf{x}(k)$  that is composed of differences between each state variable at slot  $k, \dots, k - \nu$  and their equilibrium values.

$$\mathbf{x}(k) = \begin{pmatrix} r_1(k) - r_1^* \\ \vdots \\ r_1(k - \nu) - r_1^* \\ \vdots \\ r_M(k) - r_M^* \\ \vdots \\ r_M(k - \nu) - r_M^* \\ q(k) - q^* \\ \vdots \\ q(k - \nu) - q^* \end{pmatrix} \quad (20)$$

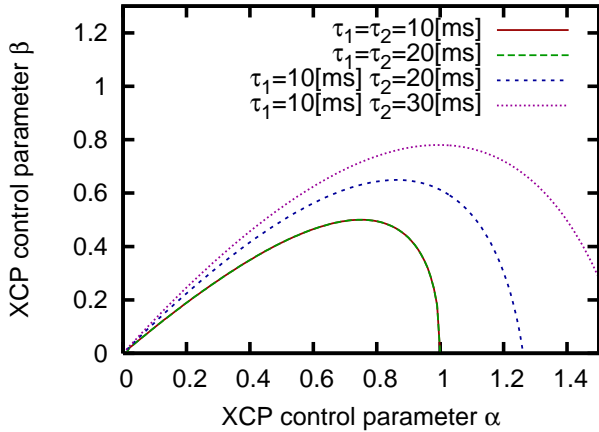


Figure 3: Stability region of XCP control parameters  $(\alpha, \beta)$  for different settings of two-way propagation delays  $(\tau_1, \tau_2)$

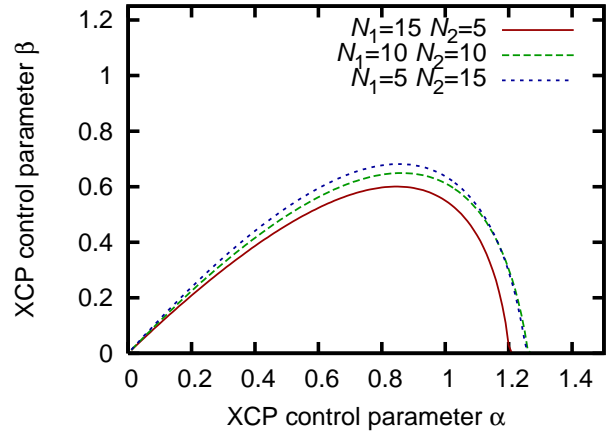


Figure 4: Stability region of XCP control parameters  $(\alpha, \beta)$  for different numbers of XCP flows in each flow class  $(N_1, N_2)$

The relation between  $\mathbf{x}(k)$  and  $\mathbf{x}(k+1)$  can be represented using a state transition matrix  $\mathbf{M}$  as

$$\mathbf{x}(k+1) = \mathbf{M} \mathbf{x}(k). \quad (21)$$

Let  $\lambda_i (1 \leq i \leq (M+1)(\nu+1))$  be the eigenvalues of the state transition matrix  $\mathbf{M}$ . The maximum absolute value of eigenvalues (i.e., maximum modulus) determines the stability around its equilibrium point. It is known that the system is stable if the maximum modulus is less than unity [8].

## 5 Numerical Examples and Simulation Results

In this section, through several numerical examples and simulation results, we investigate the effect of system parameters and XCP control parameters on stability of XCP protocol. Due to space limitation, in what follows, only results in the case of two flow classes ( $M=2$ ) are shown. Unless explicitly stated, the parameter configuration shown in Tab. 2 is used. The slot length is set to  $\Delta = \min(\tau_1, \tau_2)$ .

After examining various numerical examples of our stability analysis in Section 4, we found that the control parameter  $\gamma$  is hardly affected stability of the XCP protocol. In this paper, we therefore focus only on the effect of control parameters  $\alpha$  and  $\beta$ .<sup>1</sup>

Also, we found that the output link bandwidth  $C$  of an XCP router did not affect stability of the XCP protocol. Although the proof is not shown in this paper due to space limitation, independence of the output link bandwidth  $C$  from stability of the XCP protocol can be confirmed from the fact that expansion of Eq. (19) eliminates all  $C$ 's.

<sup>1</sup>Noted that the control parameter  $\gamma$  affects efficiency of the XCP router and fairness among XCP flows in steady state [7].

First, effect of propagation delays of XCP flows on stability of the XCP protocol is investigated. Figure 3 shows stability region of XCP control parameters  $(\alpha, \beta)$  for different settings of two-way propagation delays : i.e.,  $(\tau_1, \tau_2) = (10, 10), (20, 20), (10, 20), (10, 30)$  [ms]. The stability region is a region surrounded by the boundary line in the figure, and the vertical and the horizontal axes. XCP operates stably only when XCP control parameters  $(\alpha, \beta)$  lie in the stability region.

Figure 3 indicates that the stability in a heterogeneous case (i.e., when two-way propagation delays  $\tau_1$  and  $\tau_2$  are different) is larger than that in the homogeneous case (i.e., when two-way propagation delays  $\tau_1$  and  $\tau_2$  are identical). This phenomenon can be explained by de-synchronization of XCP flows with different propagation delays; i.e., when XCP flows have different propagation delays, variation in the transfer rate of an XCP flow is likely to be canceled by those of other XCP flows. Moreover, Fig. 3 indicates that in homogeneous cases (i.e., when two-way propagation delays of all XCP flows are identical) the stability region is independent of two-way propagation delays  $\tau_1$  and  $\tau_2$ .

From these observations, we conclude that when XCP flows are heterogeneous, XCP operates more stably than the

Table 2. The parameter configuration use in numerical examples and simulation results

$C$	400 [Mbit/s]
$\tau_1$	10 [ms]
$\tau_2$	10 [ms]
$N_1$	10
$N_2$	10
$\gamma$	0.1

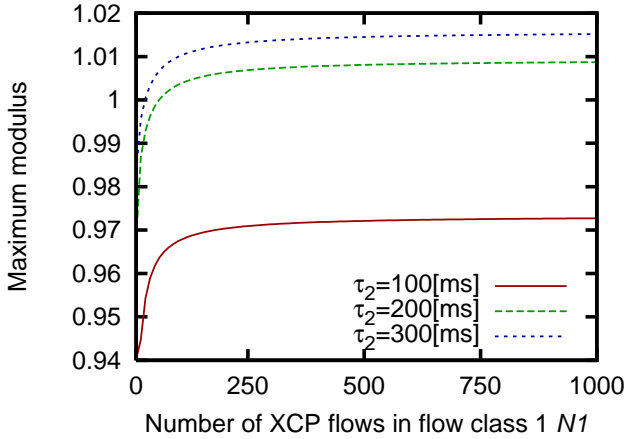


Figure 5: The maximum modulus of eigenvalues of the state transition matrix  $\mathbf{M}$  for  $\tau_1 = 10$  [ms] and  $N_2 = 1$

case when XCP flows are homogeneous.

Next, the effect of variation in propagation delays of XCP flows on stability of the XCP protocol is investigated. Figure 4 shows stability region of XCP control parameters  $(\alpha, \beta)$  for different numbers of XCP flows in each flow class: i.e.,  $(N_1, N_2) = (5, 15)$ ,  $(10, 10)$ , and  $(15, 5)$ . In this figure, propagation delays of XCP flows,  $\tau_1$  and  $\tau_2$ , are set to 10 [ms] and 20 [ms], respectively.

Figure 4 shows that the stability region is smallest when  $(N_1, N_2) = (15, 5)$ ; i.e., when the number of XCP flows in flow class 1 is larger than that in flow class 2. This phenomenon can be explained as follows. As explained in Section 2, both the efficiency controller and the fairness controller are invoked every average round-trip time of XCP flows. When there exist many XCP flows with a small propagation delay, the average round-trip time estimated by the XCP router tends to be small. Hence, the XCP router invokes the efficiency controller and the fairness controller frequently. Consequently, XCP flows with large propagation delays likely to receive too much feedback signals from the XCP router, leading unstable operation of the XCP protocol.

From these observations, we conclude that when variation in propagation delays of XCP flows are very large, operation of XCP becomes less stable.

We then investigate the effect of heterogeneity in XCP flows on stability of the XCP protocol. Figure 5 shows the maximum modulus of eigenvalues of the state transition matrix  $\mathbf{M}$  for different numbers of XCP flows in flow class 1,  $N_1$ . In this figure, the number of XCP flows in flow class 2,  $N_2$ , is fixed at one, and the propagation delay of XCP flows in flow class 1,  $\tau_1$ , is at 10 [ms]. Note that control parameters  $(\alpha, \beta)$  are set to their recommended values,  $(0.4, 0.226)$  [6].

Figure 5 shows, for example, the operation of XCP be-

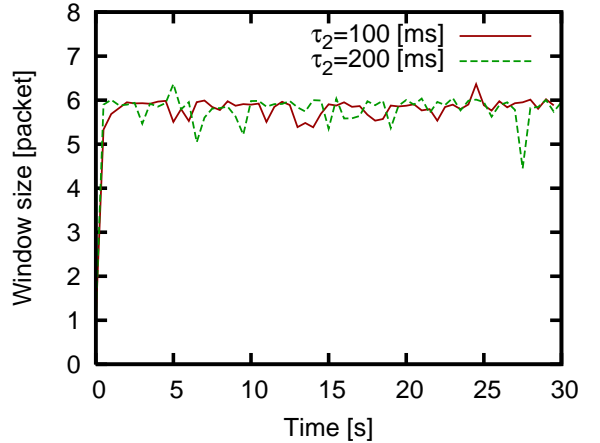


Figure 6: Evolution of the window size of an XCP flow in flow class 1 for  $\tau_1 = 10$  [ms] and  $(\alpha, \beta) = (0.4, 0.226)$

comes unstable when the number of XCP flows in flow class 1,  $N_1$ , reaches around 100 (i.e., the maximum modulus becomes larger than 1.0) for  $\tau_2 = 200$  [ms].

Finally, through simulation experiments, we confirm the validity of our stability analysis and also investigate how XCP operates unstably when the heterogeneity of XCP flows is too large. Ns-2 simulator (version 2.28) [9] is used for the following simulations. We performed simulations for the topology shown in Fig. 2. The packet size is fixed at 1,000 [byte], and the initial value of the window size is at 1 [packet].

Figures 6 through 8 show evolutions of window sizes of XCP flows in each flow class, and evolution of the queue length of the XCP router. In these figures, the number of XCP flows in each flow class,  $(N_1, N_2)$ , are set to  $(99, 1)$ . Also, the two-way propagation delay of each flow class,  $(\tau_1, \tau_2)$ , are to either  $(10, 100)$  or  $(10, 200)$  [ms].

Figures 7 and 8 indicate that, when the two-way propagation delay  $\tau_2$  of the XCP flow in flow class 2 is 200 [ms], its window size and the queue length of the XCP router show oscillatory behavior, leading low throughput. Namely, when the variation in propagation delays of XCP flows is large, the window size of the XCP flow and the queue length of the XCP router become unstable, which shows the validity of our stability analysis.

## 6 Conclusion

In this paper, we have analyzed stability of XCP in a network with heterogeneous XCP flows (i.e., XCP flows with different propagation delays). Through several numerical examples and simulation results, we have investigated the effect of system parameters and XCP control parameters on stability of the XCP protocol. Our findings include: (1)

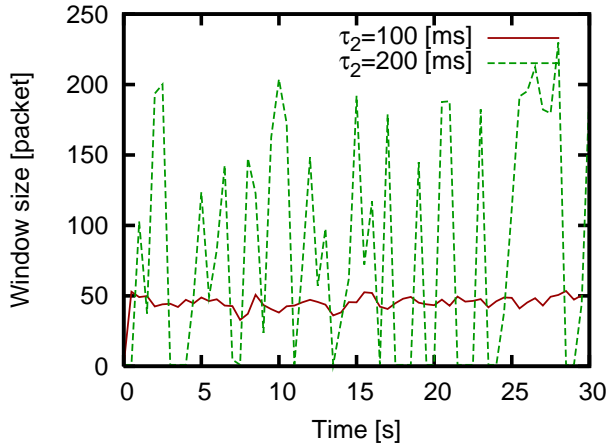


Figure 7: Evolution of the window size of an XCP flow in flow class 2 for  $\tau_2 = 10[\text{ms}]$  and  $(\alpha, \beta) = (0.4, 0.226)$

when XCP flows are heterogeneous, XCP operates more stably than the case when XCP flows are homogeneous, (2) conversely, when variation in propagation delays of XCP flows are very large, operation of XCP becomes less stable, and (3) the output link bandwidth is independent of stability of the XCP protocol.

As future work, we are planning to analyze the transient performance of XCP utilizing our fluid model of XCP derived in this paper. In addition, we are planning to derive the optimal configuration of XCP control parameters, which maximize the performance of XCP, based on our stability analysis and transient performance analysis.

## Acknowledgements

The authors would like to thank Prof. Masayuki Murata for his fruitful suggestions.

## References

- [1] H. Bulot, R. L. Cottrell, and R. Hughes-Jones. Evaluation of advanced TCP stacks on fast long-distance production networks. In *Proceedings of PFLDnet 2004*, Feb. 2004.
- [2] A. Falk and D. Katabi. Specification for the explicit control protocol(XCP). *IETF Internet Draft: draft-falk-xcp-spec-01.txt*, Oct. 2005.
- [3] S. Floyd. Highspeed TCP for large congestion windows. *Request for Comments (RFC) 3649*, Dec. 2003.
- [4] H. Hisamatsu, H. Ohsaki, and M. Murata. Fluid-based analysis of network with DCCP connections and RED routers. In *Proceedings of IEEE SAINT 2006*, pages 156–163, Jan. 2006.
- [5] D. Katabi. XCP's performance in the presence of malicious flows. In *Proceedings of PFLDnet 2004*, Feb. 2004.

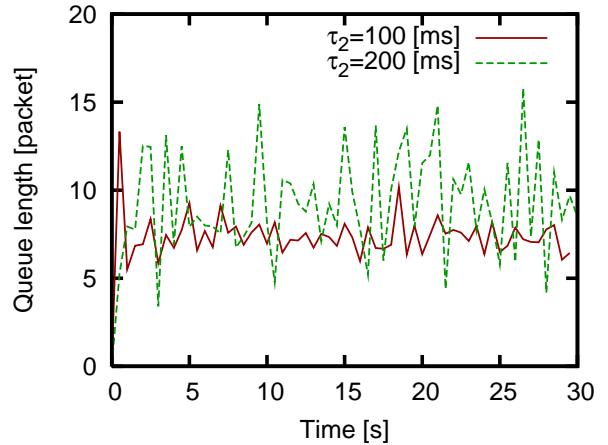


Figure 8: Evolution of the queue length of the XCP router for  $\tau_1 = 10 [\text{ms}]$  and  $(\alpha, \beta) = (0.4, 0.226)$

- [6] D. Katabi, M. Handley, and C. Rohrs. Congestion control for high bandwidth-delay product networks. In *Proceedings of ACM SIGCOMM 2002*, volume 32, pages 89–102, Aug. 2002.
- [7] S. H. Low, L. L. H. Andrew, and B. P. Wyrowski. Understanding XCP: Equilibrium and fairness. In *Proceedings of IEEE INFOCOM 2005*, volume 2, pages 1025–1036, Mar. 2005.
- [8] N. S. Nise. *Control Systems Engineering*. John Wiley & Sons, New York, 4th edition, Aug. 2003.
- [9] The network simulator – ns2. available at <http://www.isi.edu/nsnam/ns/>.
- [10] J. Padhye and S. Floyd. On inferring TCP behavior. *ACM SIGCOMM Computer Communication Review*, 31(4):287–298, Aug. 2001.
- [11] J. Postel. Transmission control protocol. *Request for Comments (RFC) 793*, Sept. 1981.
- [12] K. Ramakrishnan, S. Floyd, and D. B. Rosen. The addition of explicit congestion notification (ECN) to IP. *Request for Comments (RFC) 3168*, Sept. 2001.
- [13] L. L. Smarr, A. A. Chien, T. DeFanti, J. Leigh, and P. M. Papadopoulos. The OptIPuter. *Communications of the ACM*, 46(11):58–67, Nov. 2003.
- [14] R. Wang, G. Pau, K. Yamada, M.Y.Sanadidi, and M. Geria. TCP startup performance in large bandwidth delay networks. In *Proceedings of IEEE INFOCOM 2004*, volume 2, pages 796–805, Mar. 2004.
- [15] M. Welzl. Scalable router aided congestion avoidance for bulk data transfer in high speed networks. In *Proceedings of PFLDnet2005*, Feb. 2005.
- [16] Y. Xia, L. Subramanian, I. Stoica, and S. Kalyanaraman. One more bit is enough. In *Proceedings of ACM SIGCOMM 2005*, pages 37–48, Aug. 2005.
- [17] T. Yagi, Y. Naruse, J. Murayama, and K. Matsuda. Terabit OBS super-net experiments. *International Workshop on the Future of Optical Networking (FON)*, Mar. 2006.
- [18] Y. Zhang and M. Ahmed. A control theoretic analysis of XCP. In *Proceedings of IEEE INFOCOM 2005*, volume 4, pages 2831–2835, Mar. 2005.